

# LLM A\*: Human in the Loop Large Language Models Enabled A\* Search for Robotics

Hengjia Xiao<sup>1</sup>, Peng Wang<sup>2</sup>, Mattia Robbiani<sup>2</sup>

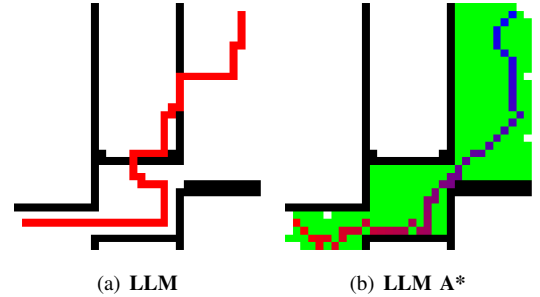
**Abstract**—This research focuses on how Large Language Models (LLMs) can help with (path) planning for mobile embodied agents such as robots, in a human-in-the-loop and interactive manner. A novel framework named LLM A\*, aims to leverage the commonsense of LLMs, and the utility-optimal A\* is proposed to facilitate few-shot near-optimal path planning. Prompts are used for two main purposes: 1) to provide LLMs with essential information like environments, costs, heuristics, etc.; 2) to communicate human feedback on intermediate planning results to LLMs. This approach takes human feedback on board and renders the entire planning process transparent (akin to a ‘white box’) to humans. Moreover, it facilitates code-free path planning, thereby fostering the accessibility and inclusiveness of artificial intelligence techniques to communities less proficient in coding. Comparative analysis against A\* and RL demonstrates that LLM A\* exhibits greater efficiency in terms of search space and achieves paths comparable to A\* while outperforming RL. The interactive nature of LLM A\* also makes it a promising tool for deployment in collaborative human-robot tasks. Codes and Supplemental Materials can be found at GitHub: <https://github.com/speedhawk/LLM-A->.

## I. INTRODUCTION

Path planning, alongside mapping, localisation, and motion planning, has long been regarded as the cornerstone technique for enabling fully autonomous agents such as robots [1]–[3]. It typically involves taking the environment map, the initial and goal states as inputs, and aims to find the (near) optimal path in terms of action costs to move the agent from the initial state to the goal state. Various approaches to path planning have been proposed, which can be classified into 1) search-based algorithms such as the classical A\* search which is guaranteed to find an optimal path when heuristics are admissible and consistent; 2) sampling-based planning such as the Rapidly-exploring Random Tree (RRT) [4] and Ant Colony Optimisation (ACO) [5], etc.; and 3) Data-driven planning such as neural A\* [6] and Reinforcement Learning (RL) based search [7].

RL is one of the most renowned data-driven planning methods. In essence, RL accomplishes path planning through trial and error. For instance, when the agent finds itself in state  $s$ , it evaluates the rewards it could receive from executing a particular action  $a$  and selects the action with the highest reward. This helps the agent to learn a ‘good’ policy that generates an obstacle-free path from the initial state to the goal state. A variety of policies have been proposed [7], with Proximal Policy Optimisation (PPO)

\*This work was supported by Manchester Metropolitan University  
Peng Wang and Mattia Robbiani are with the Department of Computing and Mathematics, Manchester Metropolitan University, Manchester, M15 6BH, UK. Hengjia Xiao is a Liverpool University graduate who participates in the work as an independent researcher. [p.wang@mmu.ac.uk](mailto:p.wang@mmu.ac.uk)



User: We have a map in which we use  $[i, j]$  to represent the node of  $i$ -th row and  $j$ -th column:  
 Start node:  $[1, 29]$ ;  
 Target node:  $[28, 1]$ ;  
 Obstacles: This map includes four obstacles respectively located at A, B, C, and D areas:  
 Region A:  $i: [0:26], j: [0:10]$ ;  
 Region B: ...  
 Agent action space:  
 Action 0: move up ( $[i, j] \rightarrow [i-1, j]$ );  
 Action 1: ...  
 Please return me all the nodes from the start node to the target node in the path planned based on A star algorithm with the measurement of Manhattan distance.

ChatGPT: Certainly! Here are all the nodes from the start node to the target node included inside the path planned using the A\* algorithm with the measurement of Manhattan distance:  
 $[(1, 29),$   
 $(1, 28),$   
 $(1, 27),$   
 $(1, 26),$   
 ...

(c) Conversation between human and LLM

Fig. 1: LLM-based path planning: (a) path planned by LLM directly; (b) path planned by the proposed LLM A\*. The initial and goal states are at the upper right and the lower left corners, respectively. The white and black tiles represent free spaces and obstacles. The red tiles form the final paths and the green tiles are the total searched tiles. We can see the path planned by LLM goes through obstacles (results generated by GPT3.5-turbo), which is prohibitive in robotics.

being among those striking a balance between convergence efficiency and stability (Schulman et al., 2017).

Although industries and academia are enthusiastic about the effectiveness of data-driven planning, these methods remain predominantly reliant on deep neural networks, making them coding-heavy and opaque (black boxes). We believe that techniques should eventually improve human welfare. Therefore, it is imperative to grant access to the underlying mechanisms of such techniques, particularly to civilian end users. This access would enable individuals to exert control or terminate certain services as needed, at any time and in any location.

Recent advancements in LLMs have facilitated a potential

overhaul of data-driven techniques. LLMs exhibit capabilities akin to human-like text generation and task completion [8]. Their generated texts consistently demonstrate adept handling of commonsense information, often to a human-like level. Particularly noteworthy is their ability to engage in a chain-of-prompts interaction, wherein humans can guide LLMs to provide desired answers. This process resembles RL apart from that the rewards are assessed and granted by humans through interaction with LLMs. These developments have somewhat diverted attention from questioning the explainability of LLMs’ underlying mechanisms, such as the ‘transformer’, a type of deep neural network. Instead, the focus has shifted towards the models’ proficiency in promptly responding to queries posed to them.

This paper harnesses the advantages of A\* being able to find an optimal path and LLMs being able to consider commonsense knowledge when interacting with humans (agents) and proposes the LLM A\*, a human-in-the-loop solution for robot path planning.

Briefly, LLM A\* can be summarised into three pivotal stages. The first stage is to set up the environment where a robot performs path planning, and communicates the information to LLMs. The second stage entails the definition of the initial state, the goal state, and the heuristics to be used. We have adopted a generic form of heuristic that considers obstacles, distances, and actions the robot can perform in the environment. It is worth mentioning that the heuristic can be tailored to specific setups based on the applications. Subsequently, LLMs identify feasible moves for path planning, evaluated against a cost function combining path cost and current-state heuristic, akin to A\*. The best ‘move’ with the minimum cost will be selected and communicated to humans upon request, who may accept or decline it. The decision will be communicated back to LLMs to carry on completing or terminating the planning. One benefit of human guidance and assessments is to minimise the use of tokens, which remains a challenge to use LLMs such as ChatGPT [8].

LLM A\* adheres to a pattern of ‘{state, action, rewards}’ that is similar to RL, yet without necessitating explicit coding, and humans have full control of the planning process. To this end, we have compared it to the advanced RL algorithm PPO for performance evaluation. A quantitative comparison with A\* is also conducted. The contributions of this paper include: 1). a first-of-its-kind LLM-based A\* is proposed for robotic path planning and a set of metrics are defined to evaluate the performance; 2). the interactive and code-free nature of LLM A\* makes it appealing to non-expert robotic users; 3). enhanced safety assurance in comparison to A\* and RL as humans are involved in the planning and loop and have full control of the planning process.

The remainder of the paper is organised as follows. Some related works are introduced in Section II. Section III elaborates on the approach. Experiments, discussions, and an ablation study are provided in Section IV, and the paper is concluded in Section V.

## II. RELATED WORK

### A. LLM for Robotic Task Planning

The concept of commanding robots through human language or instructions has been a longstanding aspiration among robotcists [9], [10]. Before the notable success of LLMs, Anderson et al. [9] introduced the R2R navigation framework, where Transformers were used to achieve visually grounded natural language navigation by translating human instructions into robot action sequences. Each action facilitated the robot’s movement from one viewpoint to another. However, details regarding how the path was planned between viewpoints were not provided, and navigation errors of up to 10 meters were reported.

Trained on (text) datasets of immense size, LLM models come with commonsense knowledge, which is promising to help accelerate robotic task planning [11]. To the best of our knowledge, most research from literature follows the visual-linguistic grounding strategy and proposes to harness the commonsense knowledge of LLMs to build a better correspondence between human language/instructions and visual perceptions of the robots. Song et al. [11] have demonstrated that LLMs can help with few-shot planning, i.e., the commonsense knowledge of LLMs is used to generate hierarchical plans, with the high-level plan being a set of viable while commonsense aligned subgoals generated by LLMs. The high-level plan is next passed to a low-level planner that is independent of the instructions to plan paths between subgoals. Other works such as [12] still fall into visual-linguistic grounding but a collision check is proposed.

It is worth noting that the works aforementioned do not delve into how LLMs can be employed to plan paths between subgoals or viewpoints. Aghzal et al. [13] introduce path planning from natural language (PPNL), emphasising the utilisation of LLMs in spatial-temporal path planning. However, their method primarily relies on prompts, lacking a connection or comparison to traditional path planning methods like A\* and RL.

### B. Reinforcement Learning for Robotic Task Planning

Reinforcement learning presents another data-driven learning-based framework for path planning. Within the RL framework, an agent endeavors to learn a policy that selects a sequence of actions leading it efficiently from one state to another, ultimately reaching the goal. This learning process is guided by a policy that rewards favorable actions while penalizing unfavorable ones.

The capacity of deep learning in data representation and processing has garnered significant attention from both the RL and robotic communities. Consequently, deep learning models have been integrated into the RL framework, giving rise to deep reinforcement learning (DRL) [14], to enable more sophisticated and effective policy learning, for robotic task planning, etc. [15].

Nevertheless, both RL and DRL still face the challenges of 1) low data efficiency that necessitates a substantial number of interactions with the environment to learn policies, as

well as the need for large datasets for training deep learning models; and 2) the stability of convergence, i.e., RL/DRL models are not guaranteed to converge. As a result, recent DRL models have focused on striking a balance between optimal states and convergence stability. The PPO model with actor-critic structures is one of the most prominent solutions. PPO is a policy gradient algorithm designed to maximise the horizon returns, while the actor-critic structure enables separate training of states and policy. This arrangement enhances planning performance and convergence of the PPO [16].

The prompt-driven LLM-based path planning can be viewed as a variant of RL models, wherein rewards are administered by humans via prompts, and policies are implicitly learned by LLMs through interactions. Consequently, we undertake a comparison of path planning performance between LLM-based methods and RL-based methods in this paper.

### III. THE LLM A\* APPROACH

#### A. Agent Path Planning Formulation

For agents like mobile robots, path planning aims to find a point-to-point utility-optimal path given an environment representation, a set of valid actions, an initial state, and a goal state. To formulate this problem, we define a graph  $\mathcal{G} = (\mathcal{S}, \mathcal{A})$ , where  $\mathcal{S}$  represents the set of states representing the environment, and  $\mathcal{A}$  represents the potentially valid actions the robot can take to move from one state to another. For instance, given two states  $(s_i, s_j) \in \mathcal{S}$ , we can define an edge  $a_{i,j} \in \mathcal{A}$ , which indicates that the agent can move from state  $s_i$  to state  $s_j$ . The cost attached to the action  $a_{i,j}$  is denoted as  $c(a_{i,j})$ .

Additionally, we define  $(s_s, s_g) \in \mathcal{S}$  as the initial state and the goal state, respectively. The output of the path planning process will be a sequence of states that form a solution path  $\mathcal{P} = (s_0, s_1, \dots, s_n)$ , where  $s_s = s_0$ ,  $s_g = s_n$ , and  $s_i \in \mathcal{S}, i = 0, 1, \dots, n$ . The path planning is carried out by iteratively expanding from the initial state, and at each state  $s$ , the valid actions will lead to a set of states  $\text{Succ}(s) \subseteq \mathcal{S}$  that could be explored next. The cumulative cost of every state  $s \in \text{Succ}(s)$  is calculated and the state to explore next is the one with the minimum cost. This process iterates until the goal  $s_n$  is reached. For a state  $s_i, i \in [0, n]$ , the cumulative cost is defined as

$$g(s_i) = \sum_{j=0}^{i-1} c(a_{j,j+1}). \quad (1)$$

The search process is designed as such to find a path  $\mathcal{P}_{\min}$  from  $s_s$  to  $s_g$  with a minimum total path cost.

#### B. Agent Path Planning with A\*

A\* is one of the most popular search-based path-planning algorithms [5]. On top of the cumulative cost, A\* exploits heuristics from priors or experiences to accelerate the search process. While the cumulative cost  $g(s_i)$  accounts for the real cost from the initial state  $s_0$  to  $s_i$ , a heuristic cost is defined

as an ‘estimate’ of the cost from  $s_i$  to the goal state  $s_n$ , which is usually denoted as  $h(s_i)$ . Considering both costs, we introduce the cost of state  $s_i$  in A\* as

$$f(s_i) = g(s_i) + h(s_i). \quad (2)$$

When the heuristic function  $h(s_i)$  is both admissible and consistent, A\* is guaranteed to find the optimal path. As a result, A\* constantly serves as a benchmark for evaluating the performance of path-planning algorithms.

#### C. Agent Path Planning with Reinforcement Learning

Path planning with RL can be represented as a graph  $\mathcal{G} = (\mathcal{S}, \mathcal{A})$ . An agent will start at an initial state  $s_0$  and learn a policy  $\pi$  through ongoing interactions with the environment. The agent will select an action  $a_{i,j}$  to traverse from state  $s_i$  to state  $s_j$ , until it reaches the goal state  $s_n$ . To maintain brevity and clarity, subscripts will be omitted hereafter.

When the agent is in a state  $s$ , we can define a state value  $V(s)$  that indicates the preference of the state. Typically, a higher value suggests a greater inclination for the agent to transition to that state.  $V(s)$  is typically represented in the form of Equation (3)

$$V(s) = \sum_a \pi(a|s)Q(s, a), \quad (3)$$

where

$$Q(s, a) = \sum_{s'} P(s', r|s, a) \left( r + \gamma V(s') \right) \quad (4)$$

is the action evaluation function that assesses an action  $a$  capable of transitioning from state  $s$  to  $s'$ ,  $P(s', r|s, a)$  is the transition probability,  $r$  is the reward of the action, and  $\gamma$  is the discount factor on state  $s'$ .  $\pi(a|s)$  is the policy to select an action from all feasible actions to complete the transition from  $s$  to  $s'$ .

The policy  $\pi$  is often parameterised by a learnable variable  $\theta$ . Equation (3) can then be reformulated as

$$J(\theta) = V^\pi(s) = \sum_a \pi_\theta(a|s)Q^\pi(s, a), \quad (5)$$

where  $J(\theta)$  is the objective function to optimise. However, Schulman et al. have shown that directly optimising equation (5) frequently results in redundant approximations and high space complexity [17]. To address this issue, Schulman et al. [18] propose an alternative objective function

$$\begin{aligned} L(\theta) &= J(\theta) - J(\theta_{\text{old}}) \\ &= \sum_s \rho_{\theta_{\text{old}}}(s) \sum_a \pi_\theta(a|s) \hat{A}_{\theta_{\text{old}}}(s, a), \end{aligned} \quad (6)$$

where

$$\hat{A}^\pi(s, a) = Q^\pi(s, a) - V^\pi(s) \quad (7)$$

is the advantage that describes the superiority of selecting an action  $a$  at state  $s$ , and  $\rho_{\theta_{\text{old}}}$  is the distribution of state  $s$  before updating the policy.

In the configuration given by Equation (6), the objective is to optimise the total advantages. The PPO model employs clip techniques to prevent significant policy changes for

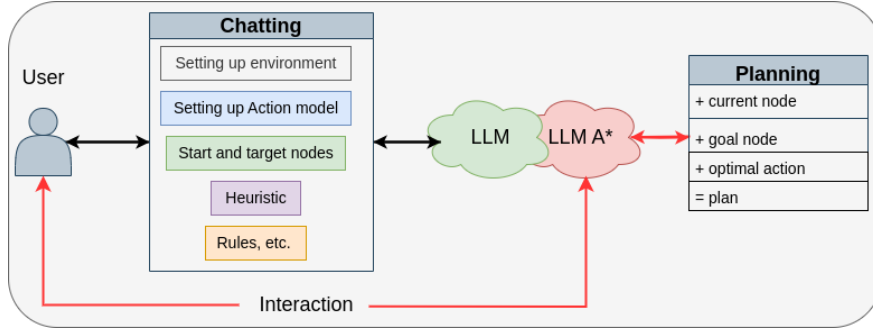


Fig. 2: The pipeline of the proposed LLM A\*. The LLM block represents the language model before the conversation with the user, and the LLM A\* block indicates that the language model is tuned to be ready to perform path planning.

```

User: We have a 32x32 grid map comprising 1024 grids in total. We use [i, j] to represent the grid in the i-th row and the j-th column. You can consider it as a binary matrix with '0' indicates the grid is free whilst '1' means the grid is occupied and the agent cannot move to it. Our objective is to make an agent at the starting node to avoid all obstacles and reach the designated target node. Considering the token limitation, please correctly and precisely remember the information above and do not return too many contexts in not only this but also the following prompts. Here is the detailed information.
LLM: .... Please proceed with the detailed information.

User: Start node: [1, 29]; Target node: [28, 1] which is at the agent's lower left direction.
LLM: echo user's message... Is there anything specific you would like assistance with regarding this scenario?

User: Obstacles: This map includes four obstacles located at region A, B, C, and D, with coordinates:
Region A: i: [0:26], j: [0:10]
Region B: i: [0:20], j: [11:21]
Region C: i: [30:31], j: [10:21]
Region D: i: [23:31], j: [21:31] except the node i=23 and j=21
LLM: echo user's message... Is there anything specific you .....?

User: Agent action space (set current coordinates of the agent to be [i, j]):
Action 0: Move up ([i, j] -> [i-1, j])
Action 1: Move down ([i, j] -> [i+1, j])
Action 2: Move right ([i, j] -> [i, j+1])
Action 3: Move left ([i, j] -> [i, j-1])
Action 4: Move upper right ([i, j] -> [i-1, j+1])
Action 5: Move upper left ([i, j] -> [i-1, j-1])
Action 6: Move lower right ([i, j] -> [i+1, j+1])
Action 7: Move lower left ([i, j] -> [i+1, j-1])

Rules:
1). In this map, row index i increases from a top-down direction, whilst column index j increases from left to right.
2). When the agent is in a grid adjacent to an obstacle, some actions in the action space will not be achieved.
3). Please dynamically adjust the agent's actions at runtime.
4). Please take the Manhattan distance from the current node to the target node into consideration for selecting next action.
LLM: Thank you for providing the description of the agent's action space. Summarising user's message ...

User: Our objective is to move the agent step by step with the actions above and avoiding the obstacles from the start node to the target node.
LLM: Summarising user's message ...

```

Fig. 3: Setting up the planning task through conversations between human users and LLMs.

better optimisation convergence control [17], [18]. In the PPO setup, Equation (6) is modified to

$$L^{clip}(\theta) = \mathbb{E} \left[ \min \left( r(\theta) \hat{A}(s, a), \text{clip}(r(\theta), 1-\epsilon, 1+\epsilon) \hat{A}(s, a) \right) \right], \quad (8)$$

where  $r(\theta) = \pi_{\theta}(a|s)/\pi_{\theta_{old}}(a|s)$  is the policy ratio that is clipped into  $[1-\epsilon, 1+\epsilon]$  with  $\epsilon$  a small number set manually.

#### D. Agent Path Planning with LLM A\*

LLM A\* is an LLM-based path-planning framework inspired by A\* and RL, to utilise commonsense knowledge

of LLMs to achieve few-shot, code-free, and near-optimal path planning for robotics. LLMs are considered code-free implicit policy learners, that learn from environment information encoded in a graph  $\mathcal{G} = (\mathcal{S}, \mathcal{A})$ , and rewards from the cost function shown in equation (2) as well as from humans who are communicating to LLMs through prompts, to accomplish path planning.

As depicted in Fig. 2, constructing an LLM A\* model primarily involves two stages. The first stage entails ‘teaching/tuning’ an LLM to comprehend the environment in which

```

User: Now, the agent is at the grid [1, 29]. Be aware of obstacles I told you and the 8 actions you can perform. All the actions should serve for the purpose of 'reaching the target node'. The agent must move in the correct direction while avoiding obstacles.
LLM: Based on the current location of the agent at grid [1, 29], and considering the obstacles and objective, I will provide you a subset of the action space that satisfies the follow criteria: Summarizing user's message on rules...

Based on these criteria, the subset of optimal actions for the next step will be determined. I will provide you a list containing the corresponding action numbers.
User: Please ONLY provide the action number list with the format 'opt_actions: [1, 2, 3]'.
LLM: opt_actions: [0, 2, 4, 5, 7]. Based on the Manhattan distance standard, next step will be moving to grid [2, 28].
User: Now, the agent is at the grid [2, 28]. The identical procedure as above...

```

Fig. 4: Robotic path planning through conversation.

the agent operates, along with the available actions it can perform. Both are encoded in a graph  $\mathcal{G} = (\mathcal{S}, \mathcal{A})$ . The initial and goal state pair  $(s_s, s_g) \in \mathcal{S}$ , heuristics, and any other relevant rules are also communicated to the LLM. One example of communicating such information to the LLM is provided in Fig. 3.

The second stage involves the path-planning process. Equipped with the requisite information, the LLM endeavors to devise a path between the initial state  $s_s$  and the goal state  $s_g$ . As prompts are employed to interact with the LLM, human intervention may be necessary during the planning phase for two purposes: 1) guiding the LLM to only convey essential information back to humans, thereby conserving valuable tokens; 2) offering guidance or heuristics when required to expedite the planning process. The prompts also empower humans to inquire about the planning process as needed, rendering the entire planning process transparent to humans. Fig. 4 illustrates how path planning is facilitated through ‘chatting’ with the LLM.

## IV. EXPERIMENTS AND DISCUSSIONS

### A. Setup

To evaluate the performance of LLM A\*, we conducted a series of experiments comparing it to A\* and RL. We considered two variants of LLM A\*:

- 1) Greedy LLM A\*, which only considers the heuristic  $h(s)$  as the cost function. To avoid ambiguity, we denote it as LLM Greedy hereafter.
- 2) LLM A\*, which considers the combination of cumulative and heuristic costs  $f(s)$  as the cost function.

The GPT3.5-turbo-16k LLM is used as it provides more tokens than GPT3.5-turbo or even GPT4. This is to ensure that we can get the planning results without disruption, not necessarily that the algorithm needs so many tokens. The GPT-3.5-turbo-16k LLM model allows for a total of 16,384 tokens, whereas GPT-3.5-turbo has a maximum of 4,096 tokens. In case there is a need to reduce the consumption of tokens to replicate the experiments, one can reset the request dictionary to null after each interaction. To enable full control/access to the planning process, one can split a

single interaction process into two stages: 1) planning by LLM A\*; and 2) outputting necessary results upon requests.

For evaluation purposes, we primarily utilise three different occupancy grid maps (which are popular in planning and navigation) denoted as Ailse, Canyon, and Double Door, respectively. Each map is of the same size  $24 \times 24$  but with different obstacle distributions. Each map consists of both free spaces and obstacles, wherein the robot agent can only traverse through free spaces while avoiding collisions with obstacles. The agent can move in eight directions at most, provided it is safe to do so. All experiments are conducted at least three times using Python 3.8+ on Google Colab, and the average results are reported. The RL model employed in our experiments is based on the PPO configuration. We use this RL model alongside the standard A\* algorithm for comparison purposes. Experiments on grid maps sized  $16 \times 16$  and  $32 \times 32$  were also conducted with results and analysis provided in the Ablation section.

### B. Evaluation Metrics

To evaluate the performance of the proposed approaches and their counterparts, we utilise three metrics: **1) The Search Complexity:** For both A\* and LLM A\*, the overall length of the open set (grids to visit) and the closed set (visited grids) maintained by the two algorithms is used as the search complexity indicator. For LLM Greedy and RL, search complexity is equivalent to the total number of grids accessed until the goal is reached. This metric is used to explore the potential of LLM in reducing search complexity. **2) The Path Length:** Measures the length of the final path found by each algorithm. **3) The Maximum Deviation Times (MDT):** The MDT serves as a measure of the smoothness of the final path and it is defined in Equation (9)

$$\text{MDT} = \sum_{t=1}^T \delta(\langle v_d, v_t \rangle), \quad (9)$$

where

$$\delta(\langle v_d, v_t \rangle) = \begin{cases} 1, & \pi/2 < \langle v_d, v_t \rangle \leq \pi \\ 0, & \text{else} \end{cases}. \quad (10)$$

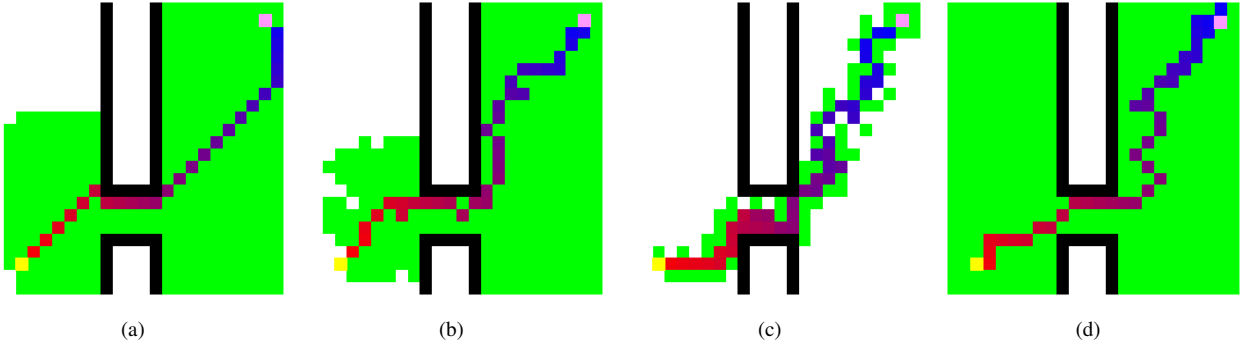


Fig. 5: Path planning results: (a), (b), (c), and (d) are results from A\*, LLM A\*, LLM Greedy, and PPO, respectively. The pink grids mark the initial states, while the yellow grids denote the goal states. White tiles depict free spaces, whereas black tiles represent obstacles. The green grids illustrate the search space. The final path is depicted by grids transitioning from blue to red, with color gradients aiding in visualising any back-and-forth movements within the paths.

In the definitions above,  $v_d$  is a directional vector that connects the initial state and the goal state and it indicates a global direction the search should expand towards.  $v_t$  is a vector originating from state  $s_{t-1}$  and terminating at state  $s_t$  and we use it to represent the direction of the agent’s movement from state  $s_{t-1}$  to  $s_t$ . We first calculate the angle  $\langle v_d, v_t \rangle$  between  $v_d$  and  $v_t$ . If the result satisfies Equation (11), it suggests that the agent is likely to move away from the goal. This can result in a longer path or a path with numerous back-and-forth movements, which undermines the smoothness of the path and is not preferred by agents such as robots.

$$\pi/2 < \langle v_d, v_t \rangle \leq \pi, \quad (11)$$

where  $\langle v_d, v_t \rangle$  is the inner product of  $v_d$  and  $v_t$ , and we use it to denote the angle between  $v_d$  and  $v_t$ . Essentially, MDT is the maximum number of times Equation (11) is satisfied when the agent moves toward the goal along the planned path.

### C. LLM A\* Training and Session Design

For experiments involving LLM, there are two stages: initialisation and interactive planning. During initialisation, essential information about the environment and the agent is prompted to be set up for planning. This includes 1) locations (coordinates) of the initial and goal states; 2) how obstacles are distributed in the environment; 3) the action space of the agent; 4) the Manhattan distance used for cumulative and heuristic cost calculation; and 5) the objective to plan a path between the initial and goal states. In addition, planning rules are communicated to LLM, such as 1) a viable path should avoid colliding with obstacles; 2) the path should ideally expand along the direction from heuristics or human guidance; 3) preference of actions that help accelerate the planning process.

In the second interactive planning stage, LLM can provide planning results based on the initial information and other prompts to assist humans in guiding or monitoring the planning process. This stage operates iteratively and interactively

until a path is successfully planned. It’s important to note that humans can request intermediate planning results at any stage, making the planning process transparent (white box) to humans and ensuring safety, among other benefits.

### D. RL Model Training

The PPO model serves as a data-driven benchmark alongside A\* for comparison. In our setup, the PPO model adopts an actor-critic structure comprising two 3-layer deep neural networks for policy and value training, respectively. The model undergoes training for 2,000 episodes, with each episode having a maximum of 200 steps to ensure convergence. To prevent premature model fixation and achieve a balance between exploration and exploitation, we set the learning rates of both the actor and critic to be smaller than 0.0005.

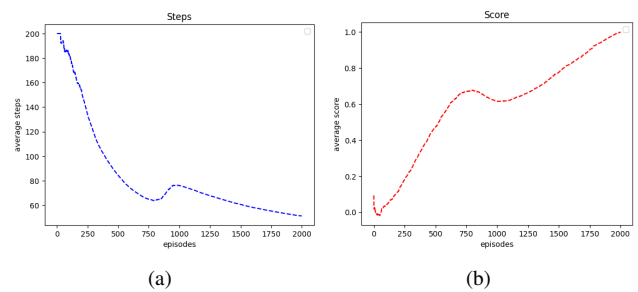


Fig. 6: Coverage of RL model training: (a) average steps per episode; (b) average scores achieved per episode.

To enhance the adaptability of the PPO model to diverse environments, we introduce a mechanism of randomising the initial state in each episode. This mechanism involves a progressive training approach, starting from states near the goal where the agent is close enough to reach it in one step. Subsequently, states are randomly selected from this subset for PPO training. As the model initially operates within a limited map scope, convergence is relatively easy.

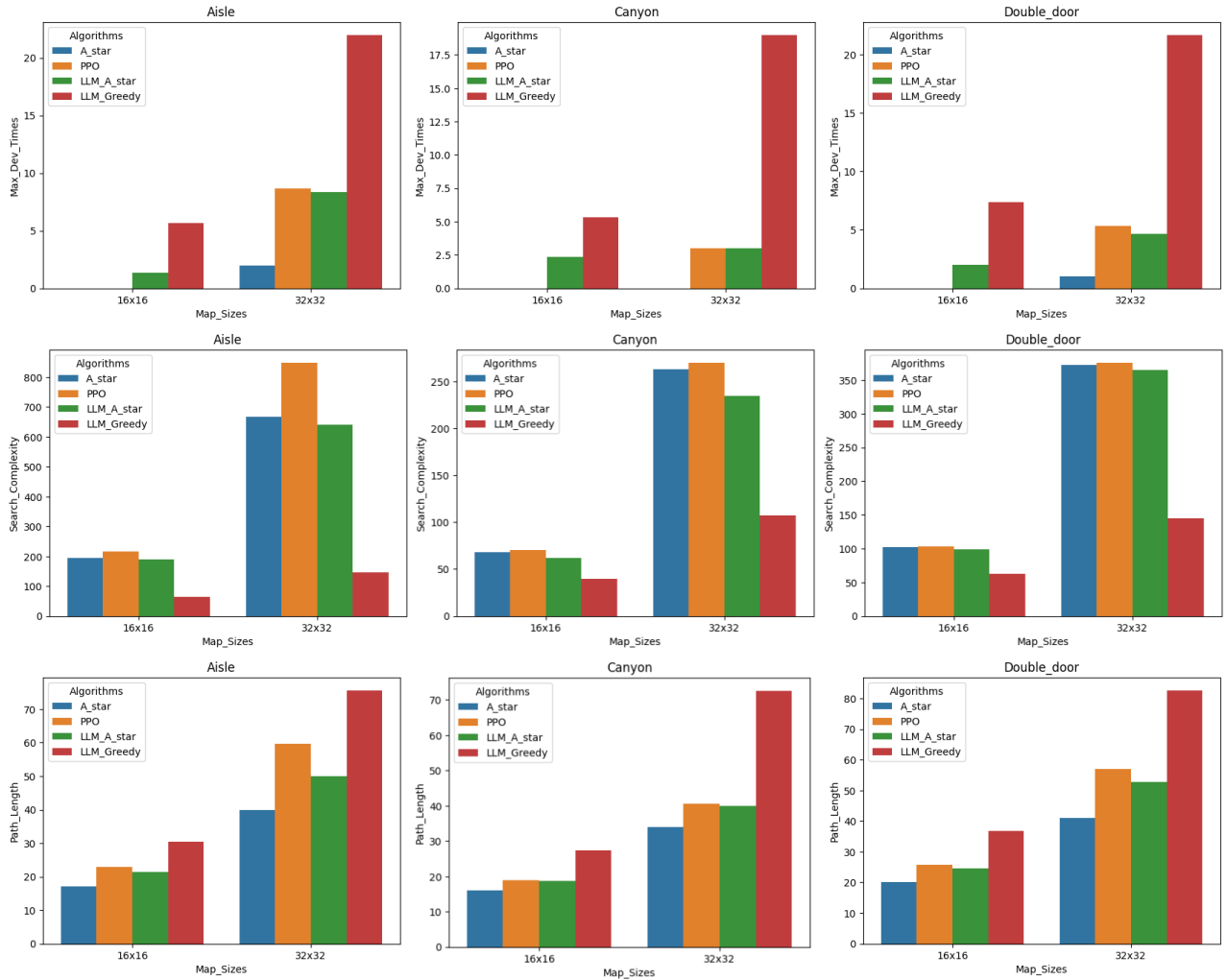


Fig. 7: Experimental results of A\*, LLM A\*, LLM Greedy, and PPO on the Aisle and Double Door environments with different sizes, i.e.,  $16 \times 16$  and  $32 \times 32$ .

We then incrementally increase the map scope during subsequent training iterations until convergence is achieved for path planning from the initial state to the goal state. This process, known as the easy-to-difficult mechanism, enables the model to balance adaptability to varying environments while efficiently converging. Fig. 6 shows the average steps and scores against episodes for the PPO model training. We can see that the PPO model converges in 2,000 episodes and the results are eventually generated from this model.

### E. Main Results

Figure 5 illustrates the visual comparison of path planning results obtained from A\*, LLM A\*, LLM Greedy, and the PPO model. It is evident that the search complexity, indicated by the green tiles, of LLM A\* is reduced compared to A\* and PPO. However, it is notable that LLM Greedy outperforms LLM A\*. This is attributed to the greedy nature of the heuristics, which consistently guides the agent towards the goal direction. However, the presence of obstacles may cause the agent to be redirected backward, resulting in back-and-forth movements in the final path, making it less efficient.

On the other hand, LLM A\* considers both cumulative and heuristic costs, leading to an expanded search space but resulting in a smoother path with fewer back-and-forth movements.

Table I shows the quantitative results achieved by each algorithm against Path Length, MDT, and Search Complexity. Notably, LLM-based algorithms demonstrate superior performance compared to PPO in all environments and maintain an advantage over A\* in most cases in terms of search complexity. In addition, LLM A\* outperforms PPO and LLM Greedy in terms of path length, achieving comparable results with A\*. However, A\* exhibits superiority in terms of path smoothness, with LLM A\* and PPO showing similar performance. Further studies have been carried out to further investigate and evaluate the performance in various environments, and the results are given in the Ablation section and the Supplemental Materials.

### F. Ablation Study

For a more comprehensive analysis of performance, additional experiments were conducted on grid maps sized

Metrics	Environments	A*	LLM A*	LLM Greedy	PPO
Path Length	Aisle	<b>27</b>	<b>34</b>	48.67	37.33
	Canyon	<b>24</b>	<b>27.67</b>	41.67	29
	Double Door	<b>31</b>	<b>37.33</b>	45.67	38
MDT	Aisle	<b>1</b>	4.67	12.33	<b>3</b>
	Canyon	<b>0</b>	2.33	7.67	<b>0.33</b>
	Double Door	<b>0</b>	3	7	<b>2.33</b>
Complexity	Aisle	372	<b>352</b>	<b>100.67</b>	471
	Canyon	145	<b>133</b>	<b>74</b>	156
	Double Door	210	<b>197.67</b>	<b>103.67</b>	214

TABLE I: Evaluation results of the algorithms against the defined metrics. Note each algorithm was executed three times and the average results are reported. The best two results are highlighted in the table.

$16 \times 16$  and  $32 \times 32$ . The results are depicted in Figure 7. It is evident that LLM A\* generally outperforms both LLM Greedy and PPO across all metrics in each environment while achieving comparable results with A\*.

Notably, there is an increasing trend in MDT for all algorithms as the size of the environment increases. However, we have observed a comparative advantage of LLM A\* over PPO as the environment size increases, indicating that the agent following the path planned by LLM A\* is less likely to experience back-and-forth movements within the final path compared to the path planned by RL. This underscores the potential of human knowledge and commonsense from LLMs to enhance path-planning outcomes in robotics.

### G. Discussion

The integration of LLMs undoubtedly leads to increased interactions between humans and AI agents. Our research has shown that by incorporating LLMs into traditional path-planning algorithms like A\*, we can achieve near-optimal path-planning results while still allowing humans to oversee the process. This represents a significant step towards making AI techniques transparent to humans and contributes to ensuring safety in human-robot interaction and collaboration.

It is important to highlight that the process of planning a path through interaction with LLMs bears a resemblance to using RL in path planning. Our findings demonstrate that leveraging commonsense knowledge from LLMs can greatly enhance path planning performance, particularly in terms of path length, path smoothness, and search complexity. This aspect will be further explored in our future work.

## V. CONCLUSIONS

This paper makes the first effort with the integration of Large Language Models (LLMs) with the classic A\* algorithm, introducing LLM A\* as a novel approach to human-in-the-loop interactive path planning for mobile embodied agents. By leveraging the inherent commonsense of LLMs and the optimality of A\*, LLM A\* achieves few-shot near-optimal path planning compared to data-driven models such as PPO. Additionally, LLM A\* offers the unique advantage of providing humans with complete access to the path-planning process, thereby enhancing safety when incorporating LLM A\* in embodied agent path planning.

Despite the notable advantages of LLM A\*, it is acknowledged that it shares similar inefficiencies (the LLM model training is data and computational resources demanding) with data-driven methods such as RL models. Future research will focus on enhancing the efficiency of LLM from both language modeling training/fine tuning and its integration with A\*, aiming to strike a balance between interactive capacity and efficiency to facilitate the real-life deployment of such models.

## REFERENCES

- [1] P. Wang, Q. Zhang, and Z. Chen, "A grey probability measure set based mobile robot position estimation algorithm," *International Journal of Control, Automation and Systems*, vol. 13, pp. 978–985, 2015.
- [2] Q. Zhang, P. Wang, and Z. Chen, "An improved particle filter for mobile robot localization based on particle swarm optimization," *Expert Systems with Applications*, vol. 135, pp. 181–193, 2019.
- [3] P. Wang, L. Mihaylova, P. Bonnifait, P. Xu, and J. Jiang, "Feature-refined box particle filtering for autonomous vehicle localisation with openstreetmap," *Engineering Applications of Artificial Intelligence*, vol. 105, p. 104445, 2021.
- [4] D. González, J. Pérez, V. Milanés, and F. Nashashibi, "A review of motion planning techniques for automated vehicles," *IEEE Transactions on intelligent transportation systems*, vol. 17, no. 4, pp. 1135–1145, 2015.
- [5] C. Carr and P. Wang, "Fast-spanning ant colony optimisation (fasaco) for mobile robot coverage path planning," *arXiv preprint arXiv:2205.15691*, 2022.
- [6] R. Yonetani, T. Tani, M. Berekatain, M. Nishimura, and A. Kanazaki, "Path planning using neural a\* search," in *International Conference on Machine Learning*. PMLR, 2021, pp. 12 029–12 039.
- [7] C. Zhou, B. Huang, and P. Fränti, "A review of motion planning algorithms for intelligent robots," *Journal of Intelligent Manufacturing*, vol. 33, no. 2, pp. 387–424, 2022.
- [8] OpenAI, "ChatGPT: Engaging openai's conversational ai," <https://openai.com/blog/chatgpt>, 2023, [Accessed on November 20, 2023].
- [9] P. Anderson, Q. Wu, D. Teney, J. Bruce, M. Johnson, N. Sünderhauf, I. Reid, S. Gould, and A. Van Den Hengel, "Vision-and-language navigation: Interpreting visually-grounded navigation instructions in real environments," in *Proceedings of the IEEE conference on computer vision and pattern recognition*, 2018, pp. 3674–3683.
- [10] C. Carr, P. Wang, and S. Wang, "A human-friendly verbal communication platform for multi-robot systems: Design and principles," *arXiv preprint arXiv:2211.09519*, 2022.
- [11] C. H. Song, J. Wu, C. Washington, B. M. Sadler, W.-L. Chao, and Y. Su, "Llm-planner: Few-shot grounded planning for embodied agents with large language models," in *Proceedings of the IEEE/CVF International Conference on Computer Vision*, 2023, pp. 2998–3009.
- [12] A. Xie, Y. Lee, P. Abbeel, and S. James, "Language-conditioned path planning," *arXiv preprint arXiv:2308.16893*, 2023.
- [13] M. Aghzal, E. Plaku, and Z. Yao, "Can large language models be good path planners? a benchmark and investigation on spatial-temporal reasoning," *arXiv preprint arXiv:2310.03249*, 2023.
- [14] V. Mnih, K. Kavukcuoglu, D. Silver, A. Graves, I. Antonoglou, D. Wierstra, and M. Riedmiller, "Playing atari with deep reinforcement learning," *arXiv preprint arXiv:1312.5602*, 2013.
- [15] C. Zhou, X. Lu, J. Dai, B. Huang, X. Liu, and P. Fränti, "Hybrid of representation learning and reinforcement learning for dynamic and complex robotic motion planning," *arXiv preprint arXiv:2309.03758*, 2023.
- [16] M. Andrychowicz, A. Raichuk, P. Stańczyk, M. Orsini, S. Girgin, R. Marinier, L. Hussenot, M. Geist, O. Pietquin, M. Michalski, *et al.*, "What matters for on-policy deep actor-critic methods? a large-scale study," in *International conference on learning representations*, 2020.
- [17] J. Schulman, F. Wolski, P. Dhariwal, A. Radford, and O. Klimov, "Proximal policy optimization algorithms," *arXiv preprint arXiv:1707.06347*, 2017.
- [18] J. Schulman, S. Levine, P. Abbeel, M. Jordan, and P. Moritz, "Trust region policy optimization," in *International conference on machine learning*. PMLR, 2015, pp. 1889–1897.